Hydrothermal Grown Nanoporous Iron Based Titanate, Fe₂TiO₅ for Light Driven Water Splitting

Prince Saurabh Bassi,[†] Sing Yang Chiam,[‡] Gurudayal,[†] James Barber,[*,†,§] and Lydia Helena Wong[*,†]

[†]School of Materials Science and Engineering, Nanyang Technological University, Singapore, 639798, Singapore

[‡]Institute of Materials Research and Engineering (IMRE), Agency of Science, Technology, and Research (A* Star), 3 Research Link, Singapore 117602, Singapore

[§]Department of Life Sciences, Imperial College London, London SW7 2AZ, U.K.

Ⓢ *Supporting Information*

ABSTRACT: We report the synthesis of iron based titanate (Fe₂TiO₅) thin films using a simple low cost hydrothermal technique. We show that this Fe₂TiO₅ works well as a photoanode for the photoelectrochemical splitting of water due to favorable band energetic. Further characterization of thin films including band positions with respect to water redox levels has been investigated. We conclude that Fe₂TiO₅ is a promising material comparable to hematite for constructing PEC cells.

KEYWORDS: *pseudobrookite, water oxidation, UPS, photoanode, Mott–Schottky, band levels*
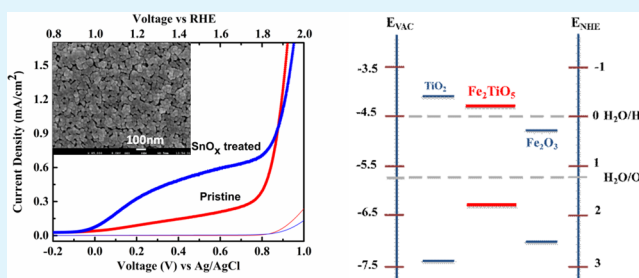
INTRODUCTION

Recently, there have been significant developments in the exploration for stable semiconductors that could be used for visible light driven water splitting,[1−4] but there have not been any suitable candidates fulfilling all the necessary requirements: to straddle fully the water oxidation/reduction potential gap, have a wide absorption of the visible solar spectrum, possess good charge transport properties, show stability (thermal and aqueous), and be nontoxic, abundant, and cheap. To overcome the common problem of inadequate band levels, photoelectrochemical cells (PEC) have been used in which an external bias is applied in addition to illumination, so as to generate both hydrogen and oxygen. Fujishima and Honda demonstrated water photolysis for the first time using the TiO₂ electrode,[5] but with a band gap of around 3 eV, it absorbs only 4% of visible light and hence is not appropriate for PEC applications. Other materials with better band gaps for water splitting like WO₃[6,7] and BiVO₄[8−10] have been studied in some depth, but over the past few years, hematite has proven to be most promising in terms of application and performance in water splitting PEC cells. It has been extensively studied owing to its favorable band gap of 2.2 eV, allowing wide absorption of visible light, good aqueous stability, low cost, and abundance in nature.[11] Hematite is predicted to achieve a water oxidation efficiency of 12.4% theoretically.[12] However, efficiencies reported are much lower due to the short carrier diffusion length (2−4 nm), poor charge transport properties, and slow oxygen evolution kinetics.[13−15] To achieve higher efficiencies, modification of hematite electrodes through nanostructuring,[16,17] elemental doping,[18] surface modification with surface passivation layers,[19−21] or introduction of cocatalysts or by

designing heterostructures have been successful approaches in recent times.[22]

Despite the many attractive features of treated nanostructured hematite as a photoanode for water oxidation, there is still a need to strive for a semiconductor material with better band positions for favorable hydrogen production and good charge transport properties to reduce the probability of charge recombination. Recently, there has been research on a plethora of hybrid photocatalysts with appropriate band level positions with complex stoichiometry or anionic tailoring that could be used for solar water splitting.[1,2]

In this regards, titanates are the group of materials which exhibit significant photocatalytic properties with different stoichiometry of elements for water splitting.[3,4] Thimsen et al. presented the experimental and theoretical aspects of mixed transition metal oxide formed after incorporation into TiO₂.[23] They reported a Fe−Ti−O system and claimed that it could be extrapolated to Ti−V−O or Ti−Ni−O systems as well. Fe was incorporated into TiO₂ to effectively tailor band gaps based on the stoichiometry of mixed oxide. A mixed iron titanate showed better band positions than hematite. Since the valence band level for the latter was already favorable for water oxidation, the shift in conduction band level toward hydrogen generation would be expected to improve the performance.

Hence, there is a need to keep exploring for a more robust, abundant, and nontoxic stable oxide-based system for overall water splitting or PEC cell applications. Hematite and TiO₂
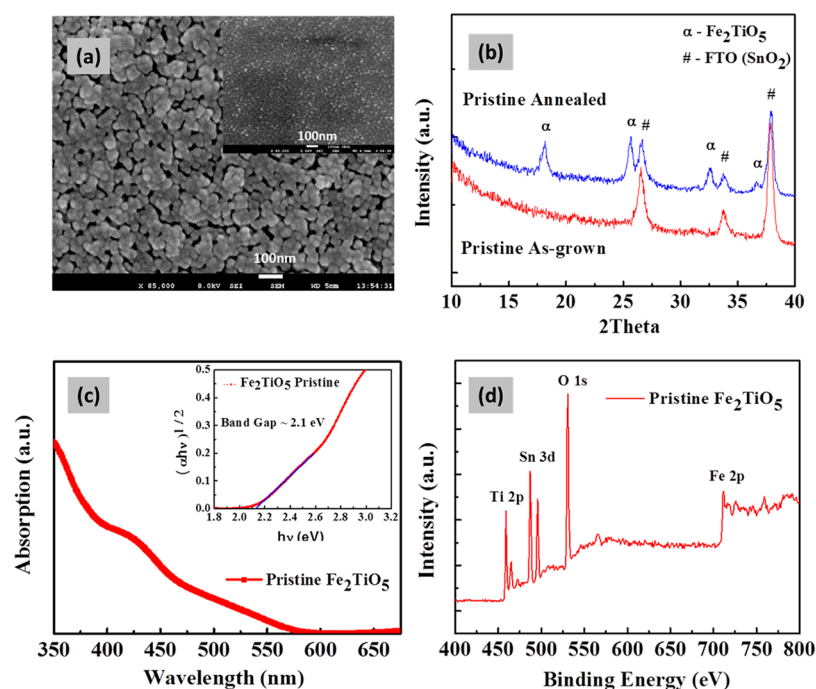
Figure 1. SEM image of (a) pristine thin film (inset: SnO_x coated film), (b) XRD pattern of samples as-grown and annealed at 750 °C, (c) UV−vis spectra of pristine films (inset: Tauc plot analysis for pristine films showing band gap around 2.1 eV), (d) XPS scan for pristine Fe_2TiO_5 annealed thin film.

being common stable oxides with light absorbing properties motivated us to work on the Fe−Ti−O system. The hybrid of Fe_2O_3 and TiO_2 could be advantageous in tackling low charge transport properties exhibited by hematite and wide band gap of TiO_2 limiting the absorption of solar spectrum. Different iron titanates $FeTiO_3$, Fe_2TiO_4, and Fe_2TiO_5 as photoanodes for photoelectrolysis of water were reported by Ginley et al.[24] Among these, $FeTiO_3$ with a band gap of 2.5−2.9 eV has been studied mainly with TiO_2 for photocatalytic applications.[25] Kim et al. reported nanodiscs of $FeTiO_3$ prepared by hydrothermal treatment which were then integrated with TiO_2 P25 nanoparticles.[26] They reported $FeTiO_3/TiO_2$ as a water oxidizing visible light photocatalyst where $FeTiO_3$ acts as the light absorber and TiO_2 as the electron transporter. Similar work has been conducted where $FeTiO_3$ is utilized as an absorption enhancing layer on TiO_2 for photochemical processes where it is also shown that valence band matching between them increases the hole transport across the semiconductor/electrolyte interface and hence enhances the photocatalytic activity.[25,27] Initially we investigated $FeTiO_3$ as a photoanode for solar driven water oxidation; but owing to the band gap of $FeTiO_3$ (∼2.5−2.9 eV), using it by itself as a photoanode results in an incomplete light absorption in the visible range. Also, Fe^{2+} oxidation states present in the material were difficult to control after high temperature annealing. Due to these factors we switched to a more stable phase Fe_2TiO_5 which is a hybrid of Fe_2O_3 and TiO_2. With a more favorable band gap of around 2.0 eV, it has a good solar spectrum absorbing qualities and is also stable in aqueous solutions.[28−30] Being a titanate, it is likely that its conduction band and valence band levels would be more favorable for water splitting as compared to hematite.[3,30] Very recently, nanoheterostructures based Fe_2TiO_5 thin films have been shown to possess favorable visible light responses even though it is hard to attribute the photoactivity to the Fe_2TiO_5 only as the produced compound

contains traces of hematite as well.[31] In this paper, we report the preparation of single phase Fe_2TiO_5 nanoporous thin films by a simple low cost hydrothermal technique and achieve a PEC performance of 0.1 mA/cm^2 for pristine films and 0.36 mA/cm^2 after surface treatment with SnO_x overlayer. Ultra-violet Photoelectron Spectroscopy (UPS) measurement has also been shown for the first time to get an insight into the band level positions with respect to vacuum energy level.

Moreover, Fe_2TiO_5 nanoporous thin films on FTO substrates were prepared by a solvothermal technique using iron(III) acetyl acetonate and titanium isopropoxide precursors in an isopropyl alcohol solution (16 mM for Fe:Ti = 2:1). To enhance the performance, surface treatment of as-grown thin films were done by drop casting 20 mM $SnCl_4·5H_2O$ solution (in ethanol). After that, the pristine and SnO_x coated photoanodes were annealed at 750 °C for 20 min at 4 °C/min. These films were characterized and investigated as photoanodes for overall water splitting. The pristine annealed thin films were also characterized for their band level positions.

■ RESULTS AND DISCUSSION

Figure 1(a) shows a top view SEM image of the pristine annealed Fe_2TiO_5 sample. The Fe_2TiO_5 nanoporous network of particles size around 30−50 nm can be observed. For the SnO_x coated sample, a very thin layer of SnO_x nanoparticles on the surface was observed as shown in the inset of Figure 1a. The presence of the additional Sn was confirmed by EDX spectroscopy. Figure 1(b) shows the XRD pattern of the films as-grown and annealed at 750 °C in air. The as-grown films were found to be amorphous, and hence only the peaks corresponding to the FTO substrates (JCPDS no. 001-0625) were observed. For a pristine annealed film, characteristic peaks from Fe_2TiO_5 (JCPDS no. 009-0182) apart from FTO can be observed which shows pseudobrookite orthorhombic Fe_2TiO_5 phase formation. The crystallite size calculated from the full
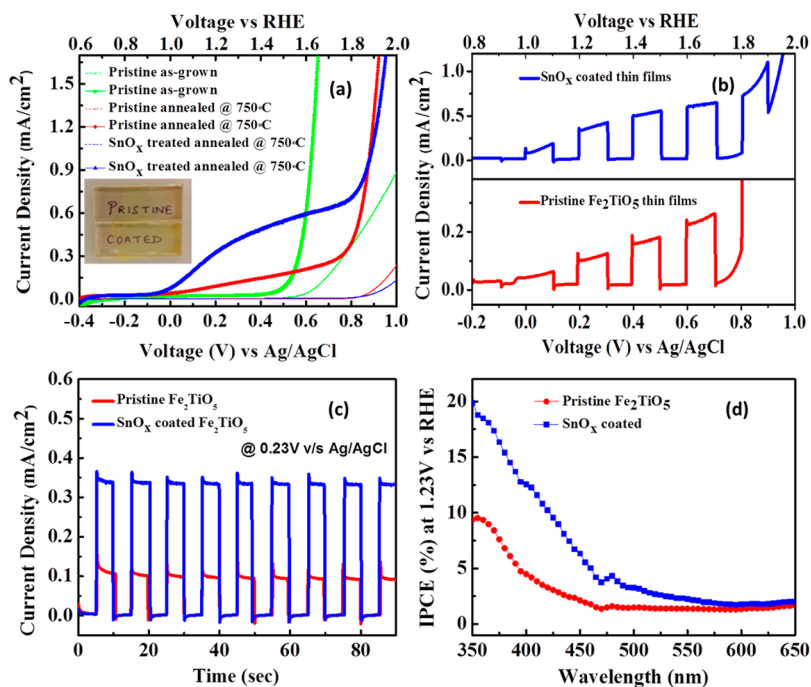
Figure 2. (a) IV curves for as-grown, pristine annealed, and SnO_x coated annealed thin films (inset: pictures of thin films) under standard AM1.5 illumination (thin/dashed curves under dark conditions), (b) IV curve under chopped light, (c) Amperometric (i-t) curves, and (d) IPCE curves for pristine and SnO_x coated films.

width half-maximum of Fe_2TiO_5 (230) peak was about 40 nm. This confirms that within the sensitivity of XRD, we obtain a single phase Fe_2TiO_5. The thickness of the film as measured from the surface profilometer was found to be around 100 nm.

Figure 1(c) is the UV−vis spectrum which shows the absorption in the visible region of the solar spectrum whose band edge was similar to hematite. Tauc plot analysis was performed, with Fe_2TiO_5 being the indirect band gap semiconductor, which yielded a band gap of around 2.1 eV which matches the previously reported value.[28]

Since SnO_2 is a wide band gap semiconductor of around 3.2 eV, the effect of overlayer did not show much effect on absorption in the visible range of the solar spectrum. To identify the presence of Fe, Ti in pristine annealed Fe_2TiO_5 thin films, XPS scan was performed as shown in Figure 1(d). Different peaks corresponding to valence states of Fe^{3+}, Ti^{4+} are shown. It should also be noted that the peak corresponding to Sn^{4+} also appears which may be the consequence of the high temperature annealing of thin films at 750 °C which allows the diffusion of Sn from FTO substrates in the semiconducting film.[13]

To evaluate the performance of Fe_2TiO_5 thin films as photoanodes for PEC applications, photoelectrochemical measurement of pristine thin films under dark and standard AM1.5G simulated conditions were performed. They showed a photocurrent (Figure 2a) of 0.1 mA/cm^2 at 1.23 V vs RHE and 0.28 mA/cm^2 at 1.75 V just before dark current onset. As shown in the inset of Figure 2a, the films are very transparent with a brownish color. These low photocurrents could therefore be attributed to a poor absorption of light. Efforts were made to overcome this problem by changing the solvothermal conditions through optimization of temperature, reaction time, and concentration of precursor solution which resulted in either a nonuniform powder-like film or did not have much effect on the thickness of the films. Prolonged

reaction times did not form the thicker film as it seemed to reach saturation after 18 h. Other efforts resulted in mixed phases with the presence of a hematite phase. It is worth noting that the solvothermal conditions were very sensitive to variations in the operating conditions which resulted in mixed phases of TiO_x or $Fe_{2-x}Ti_{1+y}O_5$-like compounds.

Surface treatment with SnO_x coating resulted in an enhancement of the photocurrent to 0.36 mA/cm^2 at 1.23 V vs RHE and 0.64 mA/cm^2 at 1.8 V just before dark current onset (Figure 2a). The improvement in the photocurrent could be attributed to the decrease in recombination of charge carriers at semiconductor/electrolyte interface through surface passivation. Figure 2b shows the photocurrent−potential curves under chopped light for pristine and SnO_x coated samples. Anodic transient signifies the holes accumulation at the semiconductor-electrolyte interface, whereas the cathodic transient is symbolic of electrons recombining with accumulated holes.[32] We observed small transient anodic photocurrents when the light was turned on which diminishes with increasing potential for coated samples. Figure 2c shows an amperometric (I-T) curve under applied voltage bias of 1.23 V vs RHE or 0.23 V vs Ag/AgCl. It should be noted that there is not much difference in the transient behavior under on and off profiles for coated and pristine samples. This seems to indicate that 1.23 V vs RHE is not enough to provide enough driving force to trapped photogenerated holes to oxidize water, but Figure 2b shows, with increasing potential, the anodic and cathodic transients both decrease after SnO_x which is consistent with passivation of surface defects. In this way, the very thin overlayer at the semiconductor/electrolyte interface improves hole transport across the interface and enhances oxygen evolution.

To measure the efficiency of solar water oxidation, the Incident Photon to Current Efficiency (IPCE) spectra were extracted for the ultraviolet−visible range of the solar spectrum
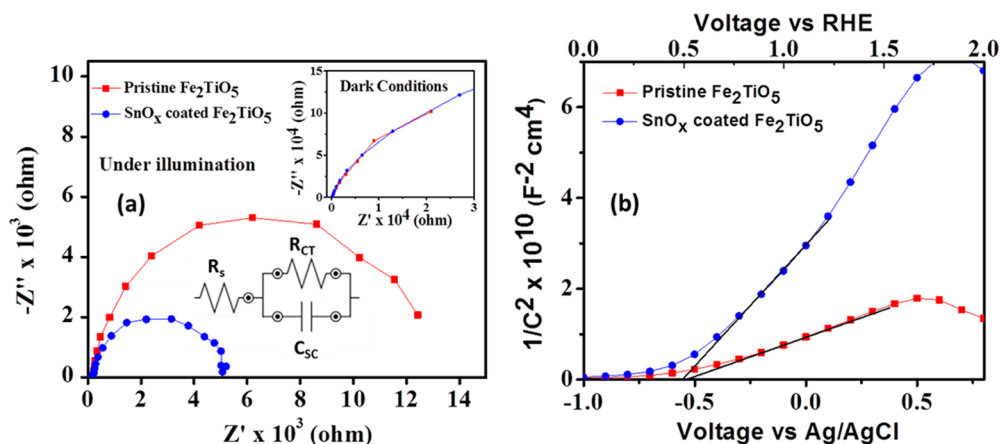
Figure 3. (a) Nyquist plots under standard AM 1.5G illumination in 1 M NaOH electrolyte (inset: under dark conditions) and (b) Mott−Schottky plots; for pristine and SnO_x coated thin films.
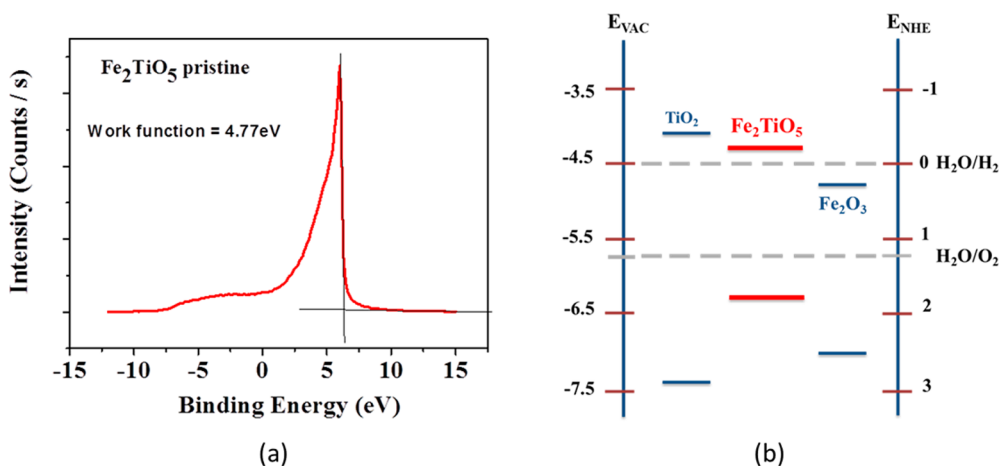
Figure 4. (a) UPS scan for pristine annealed films demonstrating evaluation of work function and (b) schematic representation of possible band level positions for Fe_2TiO_5 with respect to water redox levels.

as shown in Figure 2d. It was observed that the SnO_x coated thin films showed better efficiency than pristine thin films which corroborate the higher photocurrent pattern shown by treated samples. However, the efficiency is relatively low for both kinds of samples which may be due to inherent recombination of charges in bulk or at the semiconductor/electrolyte interface.

To investigate further into the charge transfer resistance and flat band potential, impedance spectroscopic measurements were performed for pristine and SnO_x coated films under dark and light conditions. Nyquist plots measured at 1.23 V vs RHE under illumination are shown in Figure 3a. R_s is the series resistance which depends on the external circuit dynamics, and C_{SC} is the space charge capacitance in the semiconducting layer. The charge transfer resistance (R_{CT}) for holes transport across the semiconductor-electrolyte interface was calculated after fitting the circuit as shown in Figure 3a. Under dark conditions, R_{CT} was very high of the order of 500 kΩ for pristine and 800 kΩ for coated films due to the absence of charge carriers. Under illumination, pristine films showed R_{CT} around 12.17 kΩ and 5.12 kΩ after coating. The reduction in R_{CT} after coating was evident of the increasing interfacial charge transfer rate across the semiconductor-electrolyte interface. These results were in compliance with the surface charge passivation observed with chopped light photocurrent measurement.

Hence, it further strengthens our suggestion that the SnO_x overlayer is providing a surface passivation layer. Mott−Schottky plots under dark conditions for pristine Fe_2TiO_5 and SnO_x coated Fe_2TiO_5 photoanodes extracted at 1 kHz are shown in Figure 3b. To calculate the flat band potential (V_{FB}), the following formula was used

$$1/C_{sc}^{2} = (2/\varepsilon_0\varepsilon_r e A^2 N_D)[V - V_{FB} - KT/e]$$

where ε_r is the dielectric constant for $Fe_2TiO_5(100)$, ε_0 is the permittivity of vacuum, V is the applied potential, V_{FB} is the flat band potential, KT/e is a temperature-dependent correction term (0.026 V at 25 °C), e is the elemental charge, and N_D is the dopant density (cm^{-3}). V_{FB} values for pristine and SnO_x films extracted from the above equation are 0.47 and 0.41 V vs RHE, respectively. There is a negative shift of around 60 mV after coating the samples due to the thin SnO_2 overlayer working as a surface passivation layer. It should be noted that there is an increase of slope after the treatment of pristine films. This could be due to the change in the effective surface area of the electrode which is decreasing significantly due to the thin SnO_x overlayer on porous Fe_2TiO_5 films.

To investigate the conduction band positions with respect to vacuum level (E_{vac}), UPS spectra for pseudobrookite pristine Fe_2TiO_5 thin films were evaluated. Figure 4a shows the extraction of work function (E_f) to be around 4.77 eV from the

22493

dx.doi.org/10.1021/am5065574 | ACS Appl. Mater. Interfaces 2014, 6, 22490−22495

vacuum level. Since water reduction level (E_{H2}) is 4.5 eV with respect to E_{vac}, it shows the conduction band (E_{CB}) lies in the region of hydrogen generation (see Figure 4b). Through Tauc plot analysis, the band gap was evaluated to be around 2.1 eV. Hence, it seems that the band levels of Fe_2TiO_5 straddle the oxidation/reduction levels of H_2O. This conclusion is in compliance with the earlier report on Fe_2TiO_5 where the authors deduced the band level positions with respect to hematite through their experimental data.[33] To the best of our knowledge, this is the first report of direct measurements of Fe_2TiO_5 electronic band positions using UPS.

CONCLUSIONS

In summary, we report the fabrication of Fe_2TiO_5 nanoporous thin films through a simple low cost hydrothermal technique for application in solar water splitting. The photocurrent improvement was facilitated by surface treating pristine thin films with SnO_x thin overlayer. The improvement in treated samples could be attributed to passivation of surface defects. UPS scan determined the work function and indicated that the Fe_2TiO_5 films had band level positions more favorable for water splitting as compared to hematite. Further work is required to establish if the fabrication of thicker films would result in higher performance of PEC activity in terms of hydrogen evolved due to a more complete absorption of solar light.

ASSOCIATED CONTENT

Ⓢ Supporting Information

Experimental Section, Hydrothermal Technique and Surface Modification, General Characterization, and Photoelectrochemical Characterization. This material is available free of charge via the Internet at http://pubs.acs.org.

AUTHOR INFORMATION

Corresponding Authors

*E-mail: j.barber@imperial.ac.uk.
*E-mail: lydiawong@ntu.edu.sg.

Notes

The authors declare no competing financial interest.

REFERENCES

(1) Chen, X.; Shen, S.; Guo, L.; Mao, S. S. Semiconductor-Based Photocatalytic Hydrogen Generation. *Chem. Rev.* **2010**, *110*, 6503−6570.

(2) Maeda, K.; Domen, K. Oxynitride Materials for Solar Water Splitting. *MRS Bull.* **2011**, *36*, 25−31.

(3) Walter, M. G.; Warren, E. L.; McKone, J. R.; Boettcher, S. W.; Mi, Q.; Santori, E. A.; Lewis, N. S. Solar Water Splitting Cells. *Chem. Rev.* **2010**, *110*, 6446−6473.

(4) Kudo, A.; Miseki, Y. Heterogeneous Photocatalyst Materials for Water Splitting. *Chem. Soc. Rev.* **2009**, *38*, 253−278.

(5) Fujishima, A.; Honda, K. Electrochemical Photolysis of Water at a Semiconductor Electrode. *Nature* **1972**, *238*, 37−38.

(6) Liu, X.; Wang, F.; Wang, Q. Nanostructure-Based WO_3 Photoanodes for Photoelectrochemical Water Splitting. *Phys. Chem. Chem. Phys.* **2012**, *14*, 7894−7911.

(7) Marsen, B.; Miller, E. L.; Paluselli, D.; Rocheleau, R. E. Progress in Sputtered Tungsten Trioxide for Photoelectrode Applications. *Int. J. Hydrogen Energy* **2007**, *32*, 3110−3115.

(8) Sayama, K.; Nomura, A.; Arai, T.; Sugita, T.; Abe, R.; Yanagida, M.; Oi, T.; Iwasaki, Y.; Abe, Y.; Sugihara, H. Photoelectrochemical Decomposition of Water into H_2 and O_2 on Porous $BiVO_4$ Thin-Film Electrodes under Visible Light and Significant Effect of Ag Ion Treatment. *J. Phys. Chem. B* **2006**, *110*, 11352−11360.

(9) Luo, W.; Yang, Z.; Li, Z.; Zhang, J.; Liu, J.; Zhao, Z.; Wang, Z.; Yan, S.; Yu, T.; Zou, Z. Solar Hydrogen Generation from Seawater with a Modified $BiVO_4$ Photoanode. *Energy Environ. Sci.* **2011**, *4*, 4046−4051.

(10) Abdi, F. F.; Firet, N.; van de Krol, R. Efficient $BiVO_4$ Thin Film Photoanodes Modified with Cobalt Phosphate Catalyst and W-Doping. *ChemCatChem* **2013**, *5*, 490−496.

(11) Sivula, K.; Le Formal, F.; Grätzel, M. Solar Water Splitting: Progress Using Hematite (α-Fe_2O_3) Photoelectrodes. *ChemSusChem* **2011**, *4*, 432−449.

(12) Murphy, A. B.; Barnes, P. R. F.; Randeniya, L. K.; Plumb, I. C.; Grey, I. E.; Horne, M. D.; Glasscock, J. A. Efficiency of Solar Water Splitting Using Semiconductor Electrodes. *Int. J. Hydrogen Energy* **2006**, *31*, 1999−2017.

(13) Ling, Y.; Wang, G.; Wheeler, D. A.; Zhang, J. Z.; Li, Y. Sn-Doped Hematite Nanostructures for Photoelectrochemical Water Splitting. *Nano Lett.* **2011**, *11*, 2119−2125.

(14) Sivula, K.; Zboril, R.; Le Formal, F.; Robert, R.; Weidenkaff, A.; Tucek, J.; Frydrych, J.; Gratzel, M. Photoelectrochemical Water Splitting with Mesoporous Hematite Prepared by a Solution-Based Colloidal Approach. *J. Am. Chem. Soc.* **2010**, *132*, 7436−7444.

(15) Cherepy, N. J.; Liston, D. B.; Lovejoy, J. A.; Deng, H. M.; Zhang, J. Z. Ultrafast Studies of Photoexcited Electron Dynamics in γ- and α-Fe_2O_3 Semiconductor Nanoparticles. *J. Phys. Chem. B* **1998**, *102*, 770−776.

(16) Kay, A.; Cesar, I.; Grätzel, M. New Benchmark for Water Photooxidation by Nanostructured α-Fe_2O_3 Films. *J. Am. Chem. Soc.* **2006**, *128*, 15714−15721.

(17) Kim, J. Y.; Magesh, G.; Youn, D. H.; Jang, J. W.; Kubota, J.; Domen, K.; Lee, J. S. Single-Crystalline, Wormlike Hematite Photoanodes for Efficient Solar Water Splitting. *Sci. Rep.* **2013**, *3*, 2681−2688.

(18) Gurudayal; Chiam, S. Y.; Kumar, M. H.; Bassi, P. S.; Seng, H. L.; Barber, J.; Wong, L. H. Improving the Efficiency of Hematite Nanorods for Photoelectrochemical Water Splitting by Doping with Manganese. *ACS Appl. Mater. Interfaces* **2014**, *6*, 5852−5859.

(19) Le Formal, F.; Tétreault, N.; Cornuz, M.; Moehl, T.; Grätzel, M.; Sivula, K. Passivating Surface States on Water Splitting Hematite Photoanodes with Alumina Overlayers. *Chem. Sci.* **2011**, *2*, 737−743.

(20) Xi, L.; Bassi, P. S.; Chiam, S. Y.; Mak, W. F.; Tran, P. D.; Barber, J.; Chye Loo, J. S.; Wong, L. H. Surface Treatment of Hematite Photoanodes with Zinc Acetate for Water Oxidation. *Nanoscale* **2012**, *4*, 4430−4433.

(21) Xi, L. F.; Chiam, S. Y.; Mak, W. F.; Tran, P. D.; Barber, J.; Loo, S. C. J.; Wong, L. H. A Novel Strategy for Surface Treatment on Hematite Photoanode for Efficient Water Oxidation. *Chem. Sci.* **2013**, *4*, 164−169.

(22) Bassi, P. S.; Gurudayal; Wong, L. H.; Barber, J. Iron Based Photoanodes for Solar Fuel Production. *Phys. Chem. Chem. Phys.* **2014**, *16*, 11834−11842.

(23) Thimsen, E.; Biswas, S.; Lo, C. S.; Biswas, P. Predicting the Band Structure of Mixed Transition Metal Oxides: Theory and Experiment. *J. Phys. Chem. C* **2009**, *113*, 2014−2021.

(24) Ginley, D. S.; Baughman, R. J. Preparation and Czochralski Crystal-Growth of Iron Titanates, $FeTiO_3$, Fe_2TiO_4, and Fe_2TiO_5. *Mater. Res. Bull.* **1976**, *11*, 1539−1543.

(25) Gao, B.; Kim, Y. J.; Chakraborty, A. K.; Lee, W. I. Efficient Decomposition of Organic Compounds with $FeTiO_3$/TiO_2 Heterojunction under Visible Light Irradiation. *Appl. Catal., B* **2008**, *83*, 202−207.

(26) Kim, Y. J.; Gao, B.; Han, S. Y.; Jung, M. H.; Chakraborty, A. K.; Ko, T.; Lee, C.; Lee, W. I. Heterojunction of $FeTiO_3$ Nanodisc and TiO_2 Nanoparticle for a Novel Visible Light Photocatalyst. *J. Phys. Chem. C* **2009**, *113*, 19179−19184.

(27) Truong, Q. D.; Liu, J. Y.; Chung, C. C.; Ling, Y. C. Photocatalytic Reduction of CO_2 on $FeTiO_3$/TiO_2 Photocatalyst. *Catal. Commun.* **2012**, *19*, 85−89.

(28) Enhessari, M.; Razi, M. K.; Etemad, L.; Parviz, A.; Sakhaei, M. Structural, Optical and Magnetic Properties of the Fe_2TiO_5 Nanopowders. *J. Exp. Nanosci.* **2012**, *9*, 167−176.

(29) Scaife, D. E. Oxide Semiconductors in Photoelectrochemical Conversion of Solar Energy. *Sol. Energy* **1980**, *25*, 41−54.

(30) Danzfuss, B.; Stimming, U. Iron(III)-Titanium(IV)-Oxide Electrodes: Their Structural, Electrochemical and Photoelectrochemical Properties. *J. Electroanal. Chem. Interfacial Electrochem.* **1984**, *164*, 89−119.

(31) Courtin, E.; Baldinozzi, G.; Sougrati, M. T.; Stievano, L.; Sanchez, C.; Laberty-Robert, C. New Fe_2TiO_5-Based Nanoheterostructured Mesoporous Photoanodes with Improved Visible Light Photoresponses. *J. Mater. Chem. A* **2014**, *2*, 6567−6577.

(32) Dotan, H.; Sivula, K.; Gratzel, M.; Rothschild, A.; Warren, S. C. Probing the Photoelectrochemical Properties of Hematite (α-Fe_2O_3) Electrodes Using Hydrogen Peroxide as a Hole Scavenger. *Energy Environ. Sci.* **2011**, *4*, 958−964.

(33) Bickley, R. I.; Gonzalez-Carreno, T.; Gonzalez-Elipe, A. R.; Munuera, G.; Palmisano, L. Characterization of Iron Titanium-Oxide Photocatalysts. Part 2. Surface Studies. *J. Chem. Soc., Faraday Trans.* **1994**, *90*, 2257−2264.